Proceedings of the Institute of Acoustics

VISUALISING WAVE PROPAGATION IN BIO-ACOUSTIC LENS STRUCTURES USING THE TRANSMISSION LINE MODELLING METHOD

J A Flint (1), A D Goodson (2) & S C Pomeroy (1)

(1) TLM Research Group, Department of Electronic and Electrical Engineering, Loughborough University, Loughborough, Leics., LE11 3TU, UK.
(2) Underwater Acoustics Group, Department of Electronic and Electrical Engineering, Loughborough University, Loughborough, Leics., LE11 3TU, UK.

1. INTRODUCTION

The echolocation signal generation mechanisms of dolphins and porpoises are not fully understood, although the complex morphology of the nasal passages and associated soft tissues in the forepart of the head have been intensively studied for many years. The most striking feature is the bulbous forehead comprising of lipid tissues. The systematic application of medical Computer X-ray Tomography (CT scans), Cranford [1], has now provided detailed 3 dimensional images, including tissue density data, from a variety of echolocating species and the similarities and specialisation of these internal tissues can be compared. The highly specialised lipid materials distributed within the *melon* appears to form a graded index acoustic lens. This paper describes the first use of the transmission line modelling (TLM) method for simulating the propagation of sound waves in this odontocete acoustic tissue. It presents TLM as a tool for rapid visualisation of bio-sonar emissions, and for interpreting transmission mechanisms. A basic 2D model of a melon belonging to the species *Phocoena phocoena* is evaluated, and a procedure for obtaining animated waveform visualisation is described.

2. THE TLM METHOD

TLM is a widely used time-domain numerical technique for solving a range of wave propagation problems. It was originally developed by P. B. Johns and his co-workers for solving electromagnetic wave problems in 2-dimensions [2] . A number of authors have applied the technique to solving the wave equations in acoustics, such as Pomeroy *et al.* [3] (ultrasonic imaging and inspection), and Orme *et al.* [4] (underwater acoustics). TLM can be viewed as a discretised version of Huygens' model of wave propagation, which states that every point on a given propagating wavefront acts as an isotropic secondary radiator. Each of these secondary sources act individually as spherical wavelet transmitters, and so the wave propagates by the net effect. In order to simulate this scattering process in a discretised model it is necessary to divide the space into incremental steps, Δl. Each block of space bounded by this division is modelled by a node, which is in turn composed of a number of electrical transmission lines. Waves propagate on the mesh as voltage impulses which are scattered by electrical impedance mismatches at the nodes. In acoustics problems the TLM model is analogous to the propagation of longitudinal pressure waves. The local material parameters may be appropriately adjusted in order take into account the sound velocity in a particular region. The impulses reflected from each node by the scattering process are transferred to its immediate neighbours for subsequent scattering at the next time step, Δt. Two and three dimensional problems can be successfully modelled by this method, but for simplicity only the 2D type are presented here.

3. THE BASIS OF 2D TLM MODELLING WITH SHUNT NODES

The equations for modelling acoustic waves are:

Equation 1 - Continuity equation

$$\nabla \cdot \mathbf{U} = -\sigma \frac{\partial P}{\partial t}$$

Equation 2 - Linear force equation

$$\nabla P = -\rho \frac{\partial \mathbf{U}}{\partial t}$$

where: P = acoustic pressure
U = particle velocity
σ = compressibility of the medium
ρ = equilibrium density.

If these equations are re-written in the form of a 2D wave equation, it can be shown that they are analogous to the equations of the lumped element electrical network shown in Figure 1.

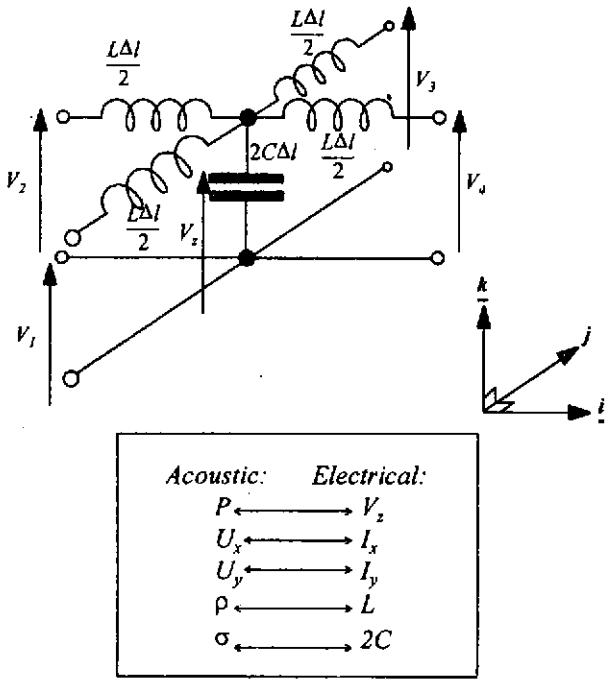

Figure 1 - Shunt node

A full derivation of the shunt node equations is detailed in [5].

The model has a wave propagation velocity of $c/\sqrt{2}$ when compared to the real world, and so it is necessary to compensate for this effect when injecting signals into the mesh. It is generally accepted that, to provide suitable accuracy, 10 nodes are required to represent each wavelength in the model at the maximum frequency and minimum sound velocity.

The scattering process can be expressed in matrix form as:

$$\begin{bmatrix} V_1 \\ V_2 \\ V_3 \\ V_4 \end{bmatrix}^r = \frac{1}{2}\begin{bmatrix} -1 & 1 & 1 & 1 \\ 1 & -1 & 1 & 1 \\ 1 & 1 & -1 & 1 \\ 1 & 1 & 1 & -1 \end{bmatrix}\begin{bmatrix} V_1 \\ V_2 \\ V_3 \\ V_4 \end{bmatrix}^i$$

The reflected voltages may thus be evaluated from the incident voltages at the previous time step. The reflected voltages are then incident voltages on adjacent nodes, and so the process continues.

4. INHOMOGENEOUS PROBLEMS

The fatty tissue in the cetacean melon requires a number of differing sound velocities which range in *Phocoena phocoena* from approximately 1246ms^{-1} in the fatty central channel to a maximum of 1435ms^{-1} where the melon is impedance matched to the water [6]. In order to model the graded index structure of the melon in TLM it is necessary to introduce additional capacitance at the node in order to modify the wave velocity. The extra capacitance is added in the form of a open circuit tuning stub. During the scattering process a portion of the voltage impulses incident on each node is transferred into the stub. At the next time step the stub impulse is injected back into the node and scatters with the incident voltages. By this means the extra capacitance required to slow the wave may be achieved. The scattering algorithm may be easily modified to account for the stub as shown below:

$$\begin{bmatrix} V_1 \\ V_2 \\ V_3 \\ V_4 \\ V_5 \end{bmatrix}^r = \frac{1}{\hat{Y}}\begin{bmatrix} 2-\hat{Y} & 2 & 2 & 2 & 2\hat{Y}_s \\ 2 & 2-\hat{Y} & 2 & 2 & 2\hat{Y}_s \\ 2 & 2 & 2-\hat{Y} & 2 & 2\hat{Y}_s \\ 2 & 2 & 2 & 2-\hat{Y} & 2\hat{Y}_s \\ 2 & 2 & 2 & 2 & 2\hat{Y}_s-\hat{Y} \end{bmatrix}\begin{bmatrix} V_1 \\ V_2 \\ V_3 \\ V_4 \\ V_5 \end{bmatrix}^i$$

Where $\hat{Y}_s$ is the normalised stub admittance, and $\hat{Y} = 4 + \hat{Y}_s$.

The admittance of the stub, $\hat{Y}_s$,is determined from the localised relative compressibility of the medium measured with respect to the compressibility of the region of space with the highest sound velocity in the model:

$$\hat{Y}_s = 4(\sigma_r - 1)$$

When the wave velocity changes at a discontinuity, it is sometimes necessary to correct the result by means of adding localised reflection coefficients. In a graded structure such as the one of interest, it should be acceptable to ignore these effects.

5. BOUNDARY DESCRIPTIONS IN TLM

Boundaries in TLM are implemented by means of terminating the outermost nodes at a distance of $\Delta l/2$ with one of the following:

1. Short circuit - representing a reflection coefficient of -1, which is used to represent boundaries to materials with a very low acoustic impedance. Pressure-release boundaries, i.e. the tissue-air boundaries around the vestibular air sacs are one such example. The boundary may be modified to take account of losses by the inclusion of a resistive component to the tuning stub.

2. Open circuit - representing a reflection coefficient of +1, which is used to represent boundaries to areas which can be considered to have infinite acoustic impedance. The bones in the model are an example of this type of boundary for a first order approximation.

3. Absorbing boundary - representing a matched condition for use on the extremities of the computational domain. Absorbing boundaries enable propagating waves to exit the problem domain without being reflected.

6. SOFTWARE

The software written has the ability to accept model data from a variety of different sources. The main input file is a 24-bit windows bitmap (.BMP) file. The colour of individual pixels within this image define the sound velocity of the materials, the boundaries, and the excitation/measuring points within the model. The program can accept up to 255 independent pressure sources which are pre-prepared as samples in a spreadsheet. Green pixels placed in the image define the excitation points, the shade of each corresponds to samples in a particular spreadsheet column. Time domain output from the mesh is automatically generated by placing red pixels on the input image. The output is stored in the columns of another spreadsheet file along with the co-ordinates of each measuring point. It is also possible to generate bitmap images as output to the mesh, which can be a useful facility for visualising wave propagation. If a number of images are produced, they may be compiled by a readily available software package into a multiple image GIF file for viewing moving pictures.

Since the program can accept standard input formats, it can utilise many commercial packages for data preparation and post processing. With the aid of such programs it has been possible to play sounds into the TLM mesh (derived from standard .WAV files) and to produce .WAV files as the output for qualitative analysis.

7. MODELLING PROCESS

In order to simulate the melon in *Phocoena phocoena*, material density information was obtained by producing a bitmap from previously published CT data [7].

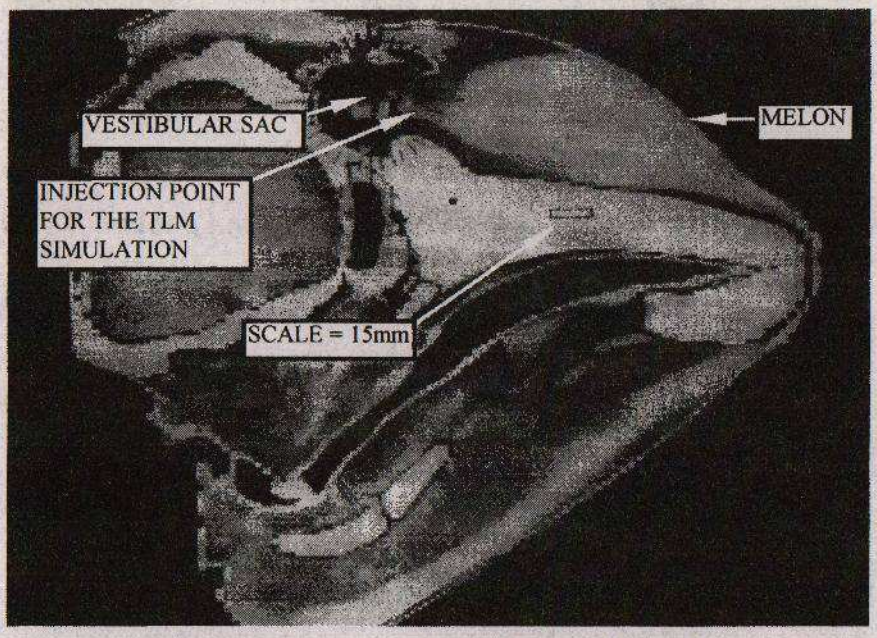

Figure 2. CT data from Cranford *et al.*

To simplify the model, the sound generation mechanism was not dealt with in the simulation. Instead a signal was injected directly into the fatty channel by using a 1.5λ (130 kHz adult centre frequency) aperture, estimated from the width of the channel, to replicate the source directivity. Figure 2 shows the data used in the simulation as published by Cranford *et al.*, along with the signal injection point. The injected signal could have been created from recorded data, but for convenience an idealised wave pattern was made in a spreadsheet to resemble that of an adult specimen (see Figure 3 and Figure 4).

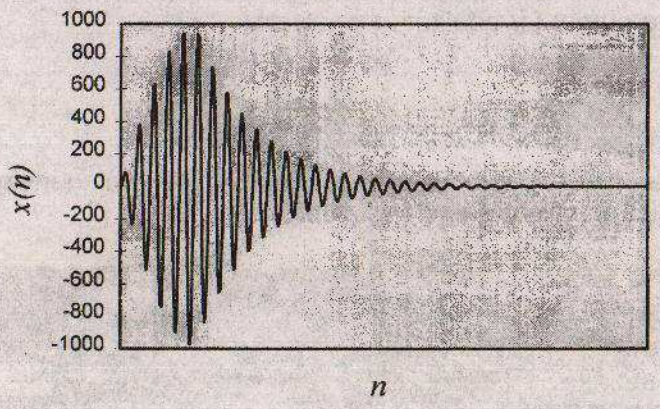

Figure 3 - Discrete time data for an idealised *Phocoena phocoena* waveform

Where:

$$x(n) = \begin{cases} A.\sin\left(\frac{n\pi}{5\sqrt{2}}\right).\sin\left(\frac{n\pi}{142}\right) & \text{for } n = 1,\ 2,\ \ldots,\ 70 \\ A.\sin\left(\frac{n\pi}{5\sqrt{2}}\right).e^{\left(\frac{t-71}{57}\right)} & \text{otherwise} \end{cases}$$

A = Amplitude of the signal
n = Iteration / sample number

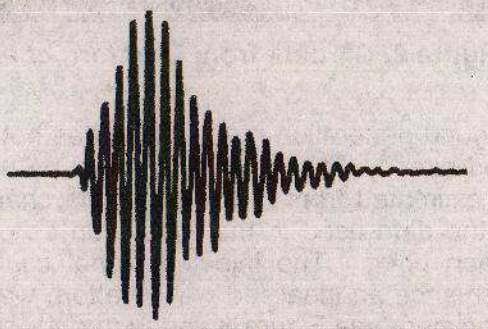

Figure 4 - Measured output of an adult *Phocoena phocoena*

The bitmap of the CT data required scaling down for use in the simulation, in order to make economical use of the processing power of the computer. As explained, the model requires at least 10 nodes for each wavelength at the frequency of interest in the TLM model, and so at 120kHz (for an adult) in the areas of the melon with the lowest sound velocity (1246ms^{-1}), 10 nodes will adequately model approximately 7mm. The diagram was resized accordingly, using the scale on the CT image as a guide. The software was modified to approximately map the densities on the CT image to sound velocities. The process was a fairly arbitrary one, since the CT data was considerably degraded through photographic reproduction. It is hoped to produce a much more accurate model in the future when the data is available in a more accurate form.

8. WAVEFORM VISUALISATION

Figure 5, Figure 6, and Figure 7 show the output from the program. The image of the skull, rostrum and soft tissues was pasted onto the simulation results to assist with the visualisation.

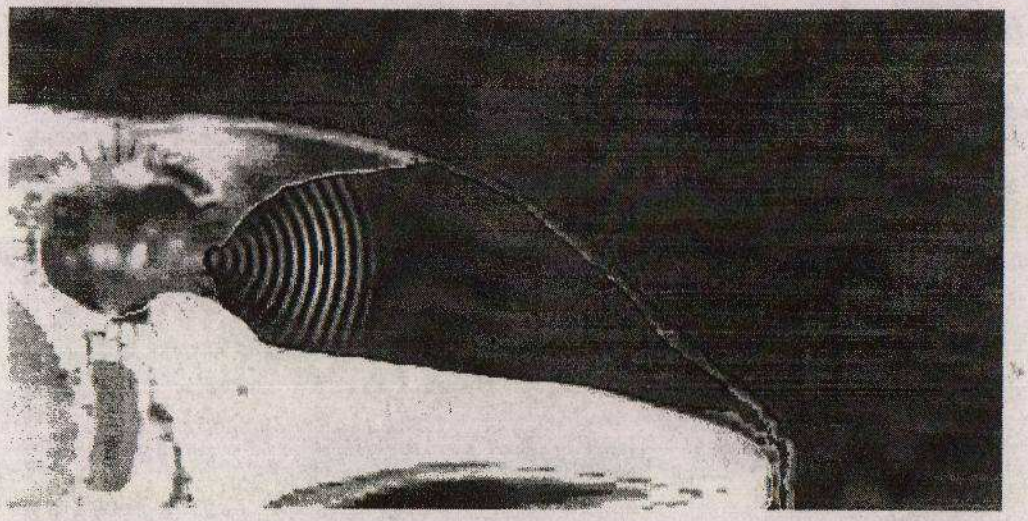

Figure 5 - Output after 200 iterations

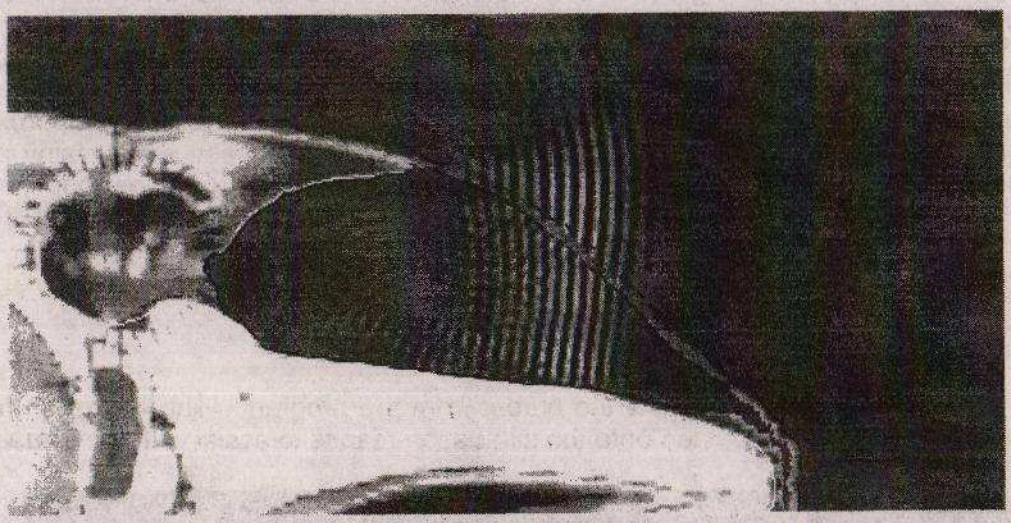

Figure 6 - Output after 490 iterations

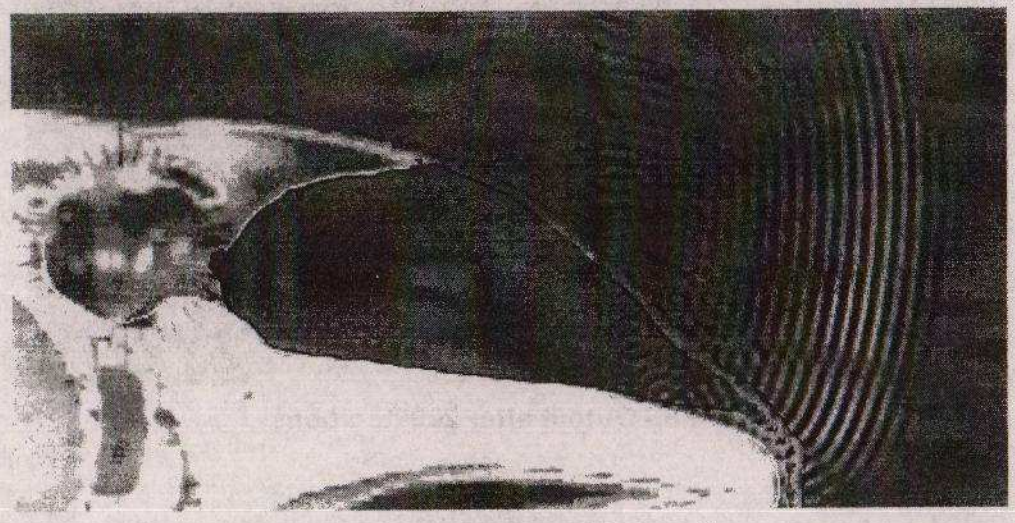

Figure 7 - Output after 770 iterations

The images clearly show the spherically spreading wavefront being flattened. The reason for this is that the sound travels faster at the edges of the melon than it does on-axis. This beam-forming allows the animal to establish far field conditions at closer ranges—a considerable advantage when intercepting small prey.

9. CONCLUSIONS

The decision to inject the output waveform at the input to the melon seems reasonable since propagation within the lens appears to be entirely refractive—the model is invalid if reflections at discontinuities occur. The model clearly does show that the that the energy is contained by the graded index waveguide effect. That the porpoise *melon* is a wave guiding structure rather than a conventional *lens* is a conclusion that appears to be supported by the finite-difference modelling techniques employed by Aroyan [8] who examined the head of a common dolphin (*Delphinus delphis*). The tissue structures prior to the melon therefore appear responsible for generating the oscillatory waveform, Goodson [9] and Amundin [10].

TLM provides a very visual means of experimenting with concepts in bio-acoustics. Its ability to model small, complex structures at close to wavelength dimensions is a particular advantage in this case.

9. ACKNOWLEDGEMENTS

The authors acknowledge the funding of the Engineering and Physical Sciences Research Council (EPSRC), and the Motor Industry Research Association (MIRA). Sincere thanks are also extended to Ted Cranford for permission to use his CT data.

10. REFERENCES

[1] T W CRANFORD 'Functional morphology of the odontocete forehead: implications for sound generation'. Doctoral thesis, University of Santa Cruz, pp272 (1992).

[2] P B JOHNS & R L BEURLE, 'Numerical solution of 2-dimensional scattering problems using a transmission line matrix', *Proceedings of the IEE*, vol. 118, no. 9, pp. 1203–1208 (1971)

[3] S C POMEROY, H R WILLIAMS & P BLANCHFIELD, 'Evaluation of ultrasonic inspection and imaging systems for robotics using TLM modelling', *Robotica*, vol. 9, pp. 283–290 (1990)

[4] E A ORME, P B JOHNS & J M ARNOLD, 'A hybrid modelling technique for underwater acoustic scattering', *International Journal of Numerical Modelling: Electronic Networks, Devices and Fields*, vol. 1, pp. 189–206 (1988)

[5] A H M SALEH & P BLANCHFIELD, 'Analysis of acoustic radiation patterns of array transducers using the TLM method', *International Journal of Numerical Modelling: Electronic Networks, Devices and Fields*, vol. 3, pp. 39–56 (1990)

[6] K S NORRIS & G W HARVEY, 'Sound transmission in the porpoise head', *Journal of the Acoustical Society of America*, vol. 56, pp. 659–664 (1974)

[7] T W CRANFORD, M AMUNDIN & K S NORRIS, 'Functional morphology and homology in the odontocete nasal complex implications for sound generation', *Journal of Morphology*, vol. 228, pp. 223–285 (1996)

[8] J L AROYAN, 'Three-dimensional numerical simulation of biosonar signal emission and reception in the common dolphin', Ph.D. dissertation, University of Santa Cruz (1996)

[9] A D GOODSON, 'A narrow band bio-sonar: investigating echolocation in the harbour porpoise, Phocoena phocoena', *Proc. Institute of Acoustics Symposium on Underwater Bio-Sonar and Bioacoustics*, (this volume) December 1997.

[10] M AMUNDIN, 'Sound production in odontocetes'. Ph.D. thesis, Stockholm University. p.144 (1991)